

Electronic Supporting Information

Plasmonic resonance enhanced photoelectrochemical aptasensor based on **g-C₃N₄/Bi₂MoO₆**

Zhenli Qiu, Jian Shu and Dianping Tang*

Key Laboratory for Analytical Science of Food Safety and Biology (MOE & Fujian Province), State Key
Laboratory of Photocatalysis on Energy and Environment, Department, Fuzhou University, Fuzhou 350116,
P. R. China.

CORRESPONDING AUTHOR INFORMATION

Phone: +86-591-2286 6125; fax: +86-591-2286 6135; e-mail: dianping.tang@fzu.edu.cn (D. Tang)

TABLE OF CONTENTS

| | |
|---|-----|
| Material and Reagent | S3 |
| Preparation of g-C ₃ N ₄ | S3 |
| Preparation of g-C ₃ N ₄ /Bi ₂ MoO ₆ | S3 |
| Preparation of Gold Nanoparticles (Au NPs)..... | S3 |
| Preparation of Au NP-Aptamer Conjugates | S4 |
| Photoelectrochemical Measurement | S4 |
| Quartz Crystal Microbalance (QCM) Measurement..... | S5 |
| Characterization of Au NP Adsorption on g-C ₃ N ₄ /Bi ₂ MoO ₆ | S6 |
| Evaluation of Aptamer-Au NPs on g-C ₃ N ₄ /Bi ₂ MoO ₆ | S6 |
| Optimization of Experimental Conditions | S7 |
| Scheme S1 and Figure S1..... | S8 |
| Figure S2 and Figure S3..... | S9 |
| Figure S4 and Figure S5..... | S10 |

■ EXPERIMENTAL SECTION

Material and Reagent. Carcinoembryonic antigen (CEA) standards from human CEA ELISA kit (Cat#: ab183365) were purchased from Abcam (Shanghai, China). Dicyandiamide ($C_2H_4N_4$), bismuth nitrate pentahydrate [$Bi(NO_3)_3 \cdot 5H_2O$], sodium molybdate dihydrate ($Na_2MoO_4 \cdot 2H_2O$), chloroauric acid ($HAuCl_4$), trisodium citrate ($Na_3C_6H_5O_7 \cdot 2H_2O$) and tris(2-carboxyethyl)phosphine (TCEP) were purchased from Sigma-Aldrich (St. Louis, MO, USA). The aptamer of target CEA used in this study was synthesized and purified by Sangon Biotech. Co., Ltd. (Shanghai, China) with the following sequence: 5'-SH-TTT TTT CCC ATA GGG AAG TGG GGG A-3'. All other chemicals employed were all of the analytical grade. Millipore water with a resistivity of $18.2 \text{ M}\Omega \text{ cm}^{-1}$ was used throughout the study. Prior to use, all the oligonucleotides were first heated to $95 \text{ }^\circ\text{C}$ for 5 min and then naturally cooled to room temperature (RT).

Preparation of g- C_3N_4 . Initially, 2.0 g of dicyandiamide powder was put into a cleaned crucible in a muffle furnace, and this sample was then heated to $550 \text{ }^\circ\text{C}$ for 4 h with a heating rate of $1.0 \text{ }^\circ\text{C min}^{-1}$. Following that, the sample was cooled to room temperature, and the obtained faint yellow g- C_3N_4 nanosheet was collected in a powder form.

Preparation of g- C_3N_4 /Bi $_2$ MoO $_6$. Initially, g- C_3N_4 samples with different masses were homogeneously dissolved into distilled water (25 mL) containing $Bi(NO_3)_3 \cdot 5H_2O$ (2.0 mmol). Thereafter, $Na_2MoO_4 \cdot 2H_2O$ (0.121 g) sample was added into the resulting mixture under vigorous stirring at room temperature. Following that, the resultant mixture was transferred into a Teflon-lined autoclave (50 mL) and heated for 12 h at $160 \text{ }^\circ\text{C}$. The product was washed for three times with deionized water and ethanol in sequence to remove the residual ions. Subsequently, the produced yellow precipitates were dried for 12 h at $60 \text{ }^\circ\text{C}$, and grinded to obtain the g- C_3N_4 /Bi $_2$ MoO $_6$. Finally, the photoelectrochemical properties of g- C_3N_4 /Bi $_2$ MoO $_6$ hybrids with the various-weight percentages were comparatively studied in detail.

Preparation of Gold Nanoparticles (Au NPs). Initially, $HAuCl_4$ aqueous solution (1.0 mL, 1.0 wt %) was added into 99-mL distilled water, and the mixture was then stirred vigorously and heated to boiling. Following that, 2.5 mL of trisodium citrate (1.0 mL, 1.0 wt %) was slowly added to the mixture and kept the liquid heated for another 15 min. Meanwhile,

the color of the solution was changed from yellow-gray to wine red. Subsequently, the resulting mixture was removed impurities by centrifugation (15 min, 14,000g). Finally, the as-prepared Au NPs were dispersed into deionized water, and stored at 4 °C for further use.

Preparation of Au NP-Aptamer Conjugates. Prior to experiment, 200 μL of gold colloids containing 150-nmol Au NPs was adjusted to pH 9.0-9.5 by using 0.1 M Na_2CO_3 aqueous solution. Then, 10 μL of the thiolated CEA aptamer (10 μM ; $\approx 100 \mu\text{mol}$) was added to gold colloids, and incubated for 16 h at room temperature (note: Before conjugation, the thiolated CEA aptamer was left into 10 mM TCEP for 1 h in order to reduce the formation of disulfide). During this process, CEA aptamers were covalently bound to gold nanoparticles *via* the dative binding between gold nanoparticles and the labeled -SH group on the aptamer. Following that, the mixture was centrifuged (14,000g) for 15 min at 4 °C. Finally, CEA aptamer-conjugated Au NPs (designated as aptamer-Au NPs) were dispersed into PBS (200 μL , 10 mM, pH 7.4), and stored at 4 °C when not in use. For comparison, the different molar ratios ($\mu\text{mol} : \text{nmol}$) of CEA aptamer and Au NP were prepared by using the same method.

Photoelectrochemical Measurement. Prior to measurement, an effective area of 28.26 mm^2 ($S \approx 28.26 \text{mm}^2$) on a cleaned fluorine-tin oxide (FTO) electrode was prepared by sticking a waterproof tape with a circle hole (6.0 mm in diameter) on the electrode. To prepare the photosensitive electrode, a g- $\text{C}_3\text{N}_4/\text{Bi}_2\text{MoO}_6$ suspension (1.0 mg mL^{-1}) in deionized water was initially dispersed with ultra-sonication for 10 min. Then the resulting suspension (20 μL) was dropped on the electrode and naturally dried in ambient air. Following that, 10 μL of the above-prepared aptamer-Au NP conjugates with different molar ratios were thrown onto the surface of g- $\text{C}_3\text{N}_4/\text{Bi}_2\text{MoO}_6$ -modified FTO electrodes, respectively, and naturally dried at 37 °C to ensure the effective immobilization of aptamer-Au NPs on the electrode. After being washed with PBS (10 mM, pH 7.4), the aptamer-Au NPs/g- $\text{C}_3\text{N}_4/\text{Bi}_2\text{MoO}_6$ -modified FTO electrodes were used for the detection of target CEA as follows. 10 μL of CEA standards with different concentrations were dropped on the modified FTO electrodes and incubated for 60 min at room temperature. After being washed as before, the photocurrents of the resulting FTO electrodes measured on a CHI 660D electrochemical workstation (Shanghai Chenhua Instruments Co. Ltd., China) by using two laser irradiations (365 nm, 550 nm) as the light sources. The photocurrent was determined in 5.0 mL Na_2SO_4

(0.1 M) solution at an applied potential of 0 V with a conventional three-electrode system by using the modified FTO electrode as the working electrode, a platinum wire electrode as the auxiliary electrode, and an Ag/AgCl reference electrode. All determinations were measured at least three times.

Quartz Crystal Microbalance (QCM) Measurement. QCM measurements were performed out on CHI 430A electrochemical quartz crystal microbalance system (Shanghai, China) controlled by a laptop under Windows environment (Scheme S1). The QCM system contained an external box with oscillator circuitry and a QCM detection cell. The cell consisted of three round Teflon pieces. The top piece was the cell top to hold reference and counter electrodes, the center piece was the cell body for solution, and the bottom piece was for mounting purpose. The quartz crystal was located between the center and bottom pieces, and the seal was through two O-rings pressed together by four screws. All the QCM gold substrates with sub-nm roughness on the gold surface were purchased from Shanghai CHI Instrument Co., Ltd (China).

The measurement principle of the QCM sensors is based on the response frequency according to the Sauerbrey equation: $\Delta f = -2.3 \times 10^{-6} f_0^2 \Delta m / A$, where Δf is the resonant frequency difference (Hz); f_0 is the basic resonant frequency of the crystal (-186.5 Hz); Δm is the mass accumulation on the crystal surface (mg); A is the Au surface area (0.196 cm²). The prepared QCM chip was first mounted one side of the detection vessel. Each of the samples to be analyzed was then introduced into the detection vessel after stabilization of resonance frequency (shift less than 1 Hz min⁻¹). The assay mainly consisted of the following steps: (i) *Modification of g-C₃N₄/Bi₂MoO₆ on gold substrate*: 20 μ L of the above-prepared g-C₃N₄/Bi₂MoO₆ suspension (1.0 mg mL⁻¹) in deionized water was initially dropped on the QCM probe and naturally dried in ambient air; and (ii) *Adsorption of aptamer-Au NPs*: 10 μ L of the above-prepared aptamer-Au NP conjugates with different molar ratios were thrown onto the surface of g-C₃N₄/Bi₂MoO₆-modified QCM probes, respectively, and naturally dried at 37 °C. The resulting QCM probes were washed with PBS (10 mM, pH 7.4) after each step. QCM measurement was carried out in 1.0-mL deionized water.

■ PARTICAL RESULTS AND DISCUSSION

Characterization of Au NP Adsorption on g-C₃N₄/Bi₂MoO₆. The adsorption of Au NPs on g-C₃N₄/Bi₂MoO₆ is confirmed by field-emission scanning electron microscopy (FESEM) and energy dispersive spectrometer (EDS), respectively (Fig. S2). Fig. S2A-B give typical FESEM images of the as-synthesized g-C₃N₄/Bi₂MoO₆ sample before (Fig. S2-A) and after (Fig. S2-B) modification with Au NPs, respectively. Vaguely, numerous gold nanoparticles were attached on the surface of g-C₃N₄/Bi₂MoO₆ (Fig. S2-B). After interaction of Au NPs with the g-C₃N₄/Bi₂MoO₆ hybrids, significantly, Au elements could be obviously observed in Fig. S2-C (curve 'a' versus curve 'b'). These results revealed that aptamer-Au NPs were adsorbed on the g-C₃N₄/Bi₂MoO₆ through their interaction.

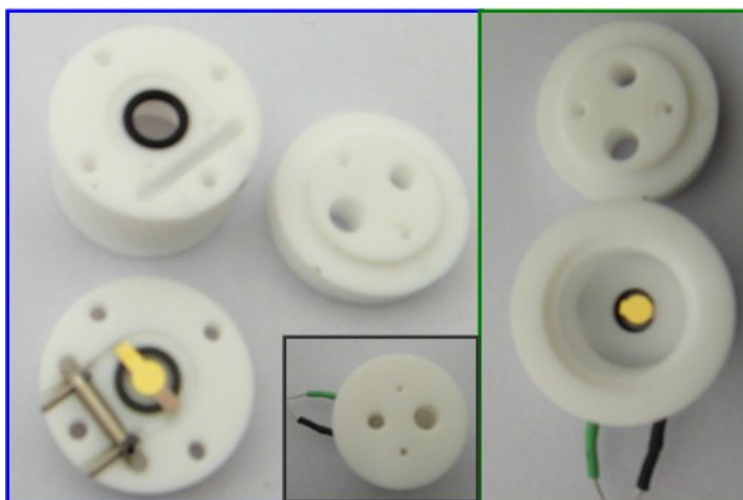
Evaluation of Aptamer-Au NPs on g-C₃N₄/Bi₂MoO₆. It is well known that QCM, as an efficient analytical tool, has been used for investigation of biomolecular interaction because of its high sensitivity, low cost, real time output, and label- or radiation-free entities. The QCM sensors measure the resonant frequency (f) using the standard oscillator technique. The frequency shift (Δf) is usually explained by the Sauerbrey equation, which states that the frequency shift is linearly proportional to the change of surface mass (Δm) on the crystal. The assay was usually implemented by the shift in the frequency before and after the interaction of the substrate with other components. Fig. S3 shows the QCM responses (frequency vs. time) of g-C₃N₄/Bi₂MoO₆ immobilization, aptamer-Au NP adsorption and target CEA introduction on the surface of QCM gold substrate, respectively. The initial baseline (background signal) was obtained when the bare QCM probe was exposed to deionized water (curve 'a'). After modification of g-C₃N₄/Bi₂MoO₆ on the QCM probe, the frequency of the substrate increased (curve 'b'). Moreover, aptamer-Au NP adsorption was remarkably observed as a result of the increase in the frequency, reflecting the kinetic process of aptamer-Au NPs adsorbed onto the gold surface (curve 'c'). The increase in the QCM frequency could be used to evaluate the amount of the aptamer-Au NPs coupled to the surface. Significantly, the frequency decreased slightly after the resulting probe reacted with 5.0 ng mL⁻¹ target CEA (curve 'd'), indicating that introduction of target CEA could induce the dissociation of aptamer-Au NPs from the surface of g-C₃N₄/Bi₂MoO₆. Unfavorably, the shift in the frequency was very weak relative to curve 'c', which did not facilitate for QCM detection in this system. According to Sauerbrey equation, however, we could calculate that the immobilized amounts of g-C₃N₄/Bi₂MoO₆ and

aptamer-Au NPs were 19.67 and 1.83 μg , respectively. In addition, these results also indicated that our strategy could be utilized for the detection of target CEA.

Optimization of Experimental Conditions. To achieve a high-sensitive PEC aptasensor with a low detection limit, several experiment parameters including the mass ratio between g- C_3N_4 and Bi_2MoO_6 , the molar ratio between CEA aptamer and Au NPs, and the incubation time of CEA with the aptamer should be investigated in detail (Fig. S4). It is generally recognized that a high photocurrent derives from the efficient electrons-holes separation in materials. Fig. S4-A shows the photocurrent-time response curves of the different-ratio g- $\text{C}_3\text{N}_4/\text{Bi}_2\text{MoO}_6$ composites with an on-off UV and visible irradiation, respectively. The photocurrent of 25 wt % g- C_3N_4 in the g- $\text{C}_3\text{N}_4/\text{Bi}_2\text{MoO}_6$ composites (1:3, w/w) was higher than those of other ratios between g- C_3N_4 and Bi_2MoO_6 under UV and visible irradiations, which is completely in accordance with the fluorescence spectrum that indicate the ability of electron-hole recombination. Thus, 1:3 (w/w) of g- C_3N_4 and Bi_2MoO_6 was selected for the preparation of g- $\text{C}_3\text{N}_4/\text{Bi}_2\text{MoO}_6$ composites in this work.

As mentioned above, the photocurrent originated from plasmonic enhancement between gold nanoparticles and g- $\text{C}_3\text{N}_4/\text{Bi}_2\text{MoO}_6$, whereas the aptamer-Au NPs were attached onto the composites by the interaction of CEA aptamer with the g- $\text{C}_3\text{N}_4/\text{Bi}_2\text{MoO}_6$. Therefore, the aptamer-Au NPs as the CEA recognition probe has a key factor relative to the photocurrent response. The molar ratio of aptamer labeled on the Au NPs would affect the sensitivity of PEC aptasensor. As displayed in Fig. S4-B, an optimal photocurrent response was acquired at the molar ratio of 2:3 between CEA aptamer and Au NPs in the UV and Vis irradiation. Thus, 2:3 of the molar ratio between CEA aptamer and Au NPs was employed for the fabrication of aptamer-Au NPs.

By the same token, we also investigated the effect of incubation time between the aptamer and target CEA on the photocurrent of this system. Generally, it takes some time to implement the aptamer-CEA reaction. As shown Fig. S4-C, the photocurrent reached a plateau after 60 min. A longer incubation time did not significantly change the photocurrent. To save the assay time, 60 min was employed as the aptamer-CEA reaction throughout this work.



Scheme S1 QCM measurement setup.

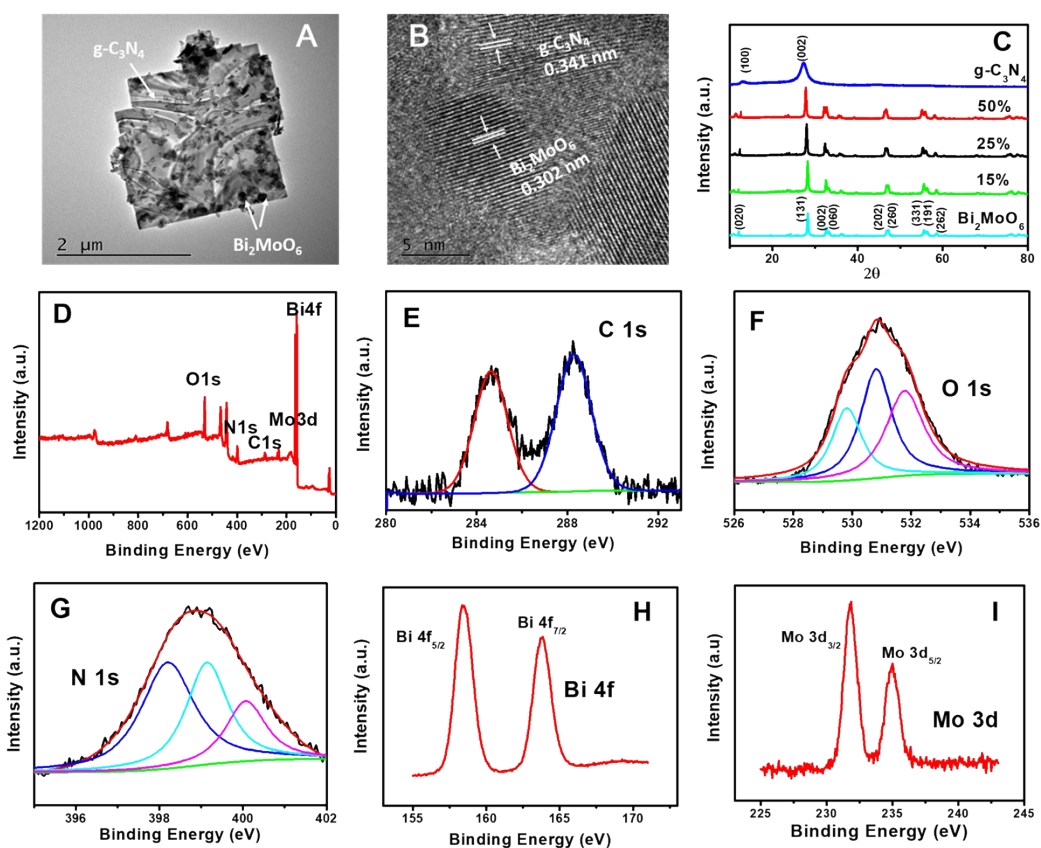


Fig. S1 (A) TEM and (B) HRTEM images of $g\text{-C}_3\text{N}_4/\text{Bi}_2\text{MoO}_6$ (1:3, w/w); (C) XRD patterns of $g\text{-C}_3\text{N}_4$, $g\text{-C}_3\text{N}_4/\text{Bi}_2\text{MoO}_6$ (1:1, w/w; 50% $g\text{-C}_3\text{N}_4$), $g\text{-C}_3\text{N}_4/\text{Bi}_2\text{MoO}_6$ (1:3, w/w; 25% $g\text{-C}_3\text{N}_4$), $g\text{-C}_3\text{N}_4/\text{Bi}_2\text{MoO}_6$ (3:17, w/w; 15% $g\text{-C}_3\text{N}_4$) and Bi_2MoO_6 from top to bottom; (D) XPS spectra of $g\text{-C}_3\text{N}_4/\text{Bi}_2\text{MoO}_6$ (1:3, w/w); (E-I) The corresponding high-resolution XPS spectra of (E) C 1s, (G) N 1s, (H) Bi 4f and (I) Mo 3d orbitals, respectively.

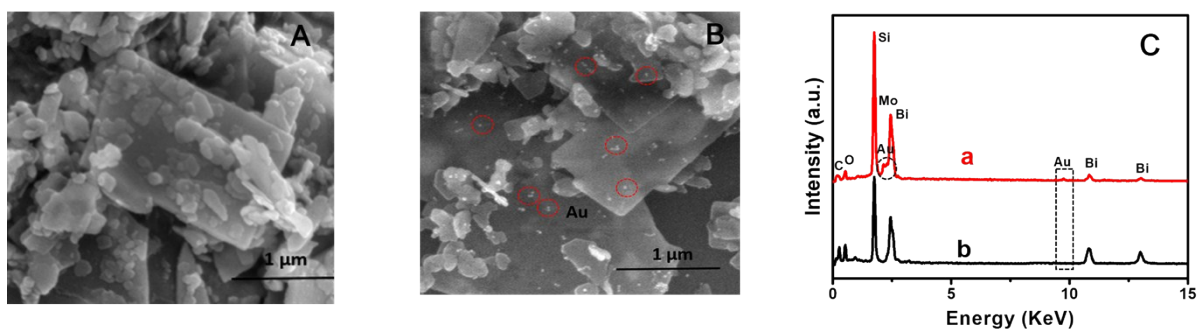


Fig. S2 SEM images of (A) g-C₃N₄/Bi₂MoO₆ (1:3, w/w) and (B) aptamer-Au NPs/g-C₃N₄/Bi₂MoO₆; (C) EDS spectra of (a) aptamer-Au NPs/g-C₃N₄/Bi₂MoO₆ and (b) g-C₃N₄/Bi₂MoO₆.

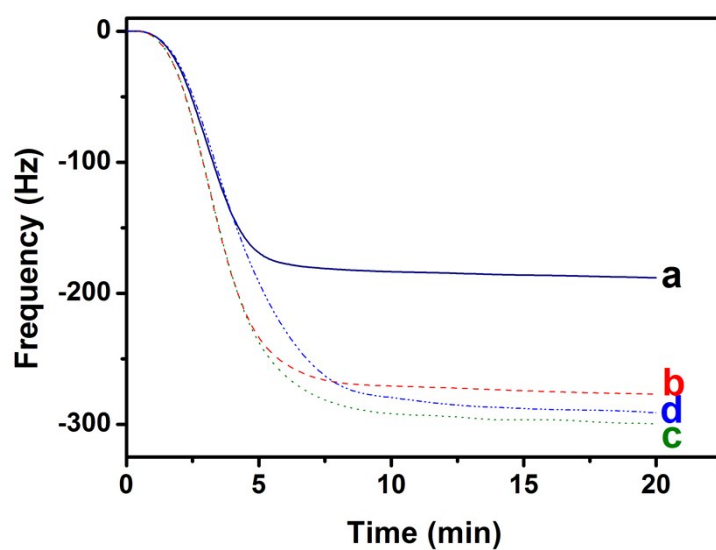


Fig. S3 QCM (frequency vs. time) measurements of differently modified gold substrates: (a) bare gold substrate, (b) g-C₃N₄/Bi₂MoO₆-modified probe 'a', (c) aptamer-Au NPs-modified probe 'b' and (d) probe 'c' after interaction with 5.0 ng mL⁻¹ target CEA.

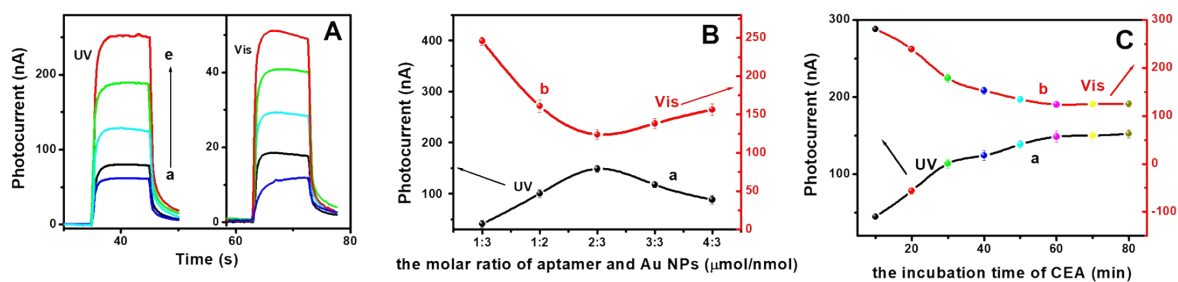


Fig. S4 Effects of (A) g-C₃N₄/Bi₂MoO₆ with different mass ratios (w/w): (a) Bi₂MoO₆, (b) g-C₃N₄, (c) g-C₃N₄/Bi₂MoO₆ (1:1, w/w; 50% g-C₃N₄), (d) g-C₃N₄/Bi₂MoO₆ (3:17, w/w; 15% g-C₃N₄) and (e) g-C₃N₄/Bi₂MoO₆ (1:3, w/w; 25% g-C₃N₄); (B) different molar ratios between CEA aptamer and Au NPs (μmol : nmol) for preparation of aptamer-Au NPs; and (C) incubation time of target CEA with aptamer-Au NPs/g-C₃N₄/Bi₂MoO₆/FTO on the photocurrent of this aptasensing platform under UV and Vis light irradiation, respectively (5.0 ng mL⁻¹ CEA used in these cases).

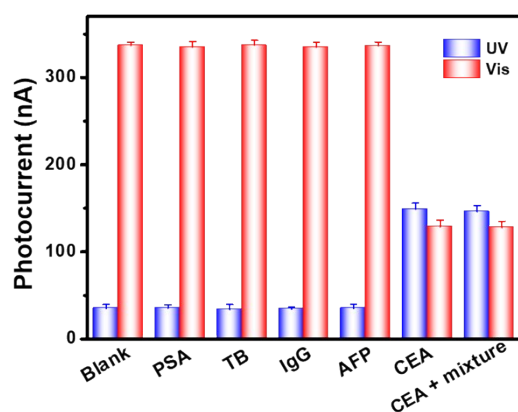


Fig. S5 Selectivity of plasmonic PEC aptasensor for 5.0 ng mL⁻¹ CEA detection against other interferences including alpha-fetoprotein (AFP; 500 ng mL⁻¹), prostate specific antigen (PSA; 500 ng mL⁻¹), thrombin (TB; 500 ng mL⁻¹), and human IgG (IgG; 500 ng mL⁻¹) under UV and Vis light irradiation, respectively (note: The mixture contained the above-mentioned analytes).